Electronic Support Information for: Temperature dependence of x-ray absorption and nuclear magnetic resonance spectra: probing quantum vibrations of light element in oxides

1 Computational details

Table 1: Parameterization of the ultrasoft (US) and Troullier-Martin [1] norm-conserving (NC) pseudopotentials. The core radii of the valence states, indicated in parentheses, are in Bohr units. The asterisk indicates that an equivalent pseudopotential has also been generated with only one $1s$ electron to serve as absorbing atom in XANES calculations

Nucleus	Type	Valence configuration	Local part
Mg*	US	$3s^2(2.50)\ 3p^0(2.60)\ 3d^{-2}(2.30)$	d
Mg	NC	$3s^1(2.50)\ 3p^0(2.50)\ 3d^0(2.50)$	d
Al*	US	$3s^2(2.10)\ 3p^1(2.10)\ 3d^{-2}(1.90)$	d
Al*	NC	$3s^2(2.00)\ 3p^{0.3}(2.00)\ 3d^{0.2}(2.00)$	d
Si*	US	$3s^2(2.10)\ 3p^2(2.10)\ 3d^{-2}(2.00)$	d
Si	NC	$3s^2(2.00)\ 3p^{1.3}(2.00)\ 3d^{0.2}(2.00)$	d
O	US	$2s^2(1.35)\ 2p^3(1.35)\ 3d^{-2}(1.3)$	d
O	NC	$2s^2(1.45)\ 2p^3(1.45)$	p

Table 2: Computational details of the DFT calculations. The coordination number of the probed atom is indicated between parentheses. For each calculation, the **k**-point mesh sampling the first Brillouin zone is given. For each compound, the phonon calculation **q**-point grid is commensurable with the supercell size used thereafter in NMR or XANES calculation. The cut-off energies E_{cut} and XANES broadening parameters γ are expressed in Ry and eV, respectively, and N_c is the total number of configurations generated to achieve convergence of temperature-dependent XANES spectra. Long-range electrostatic interactions occurring in insulators are also taken into account [2].

Mineral	Atom	Phonons		N_c	NMR			XANES			
		E_{cut}	**k**-points		Supercell	E_{cut}	**k**-points	Supercell	E_{cut}	**k**-points	γ
Periclase	Mg (6)	45	$4\times4\times4$	30	$2\times2\times2$	90	$2\times2\times2$	$3\times3\times3$	45	$3\times3\times3$	0.5
Spinel	Mg (4)	60	$2\times2\times2$	40	$2\times2\times2$	90	$1\times1\times1$	$2\times2\times2$	60	$3\times3\times3$	0.5
Spinel	Al (6)	60	$2\times2\times2$	40	$2\times2\times2$	90	$1\times1\times1$	/	/	/	/
Corundum	Al (6)	45	$3\times3\times3$	50	$2\times2\times2$	100	$1\times1\times1$	$2\times2\times2$	60	$4\times4\times4$	0.3
Berlinite	Al (4)	100	$2\times2\times2$	30	$2\times2\times1$	100	$2\times2\times2$	$2\times2\times1$	60	$3\times3\times3$	0.3
Stishovite	Si (6)	95	$3\times3\times3$	40	$3\times3\times4$	95	$1\times1\times1$	$3\times3\times4$	45	$3\times3\times3$	0.4
Quartz	Si (4)	100	$3\times3\times3$	40	$2\times2\times2$	100	$1\times1\times1$	$2\times2\times2$	45	$3\times3\times3$	0.4

The electronic sampling is done on an uniform Monkhorst-Pack **k**-points grid [3], expanding plane-waves up to an energy cut-off E_{cut}. For each compound, the dynamical matrix of the bulk unit cell

are first calculated on a wavevector grid of **q**-points commensurate with the supercell used thereafter in NMR or XANES calculations. The corresponding dynamical matrix of the supercell is then used to generate the temperature-dependent stochastic nuclear configurations.

2 Finite size effects

To demonstrate that the chosen supercell configurations are large enough, Fig. 1 displays XANES and NMR data computed at 300 K for the largest supercell sizes.

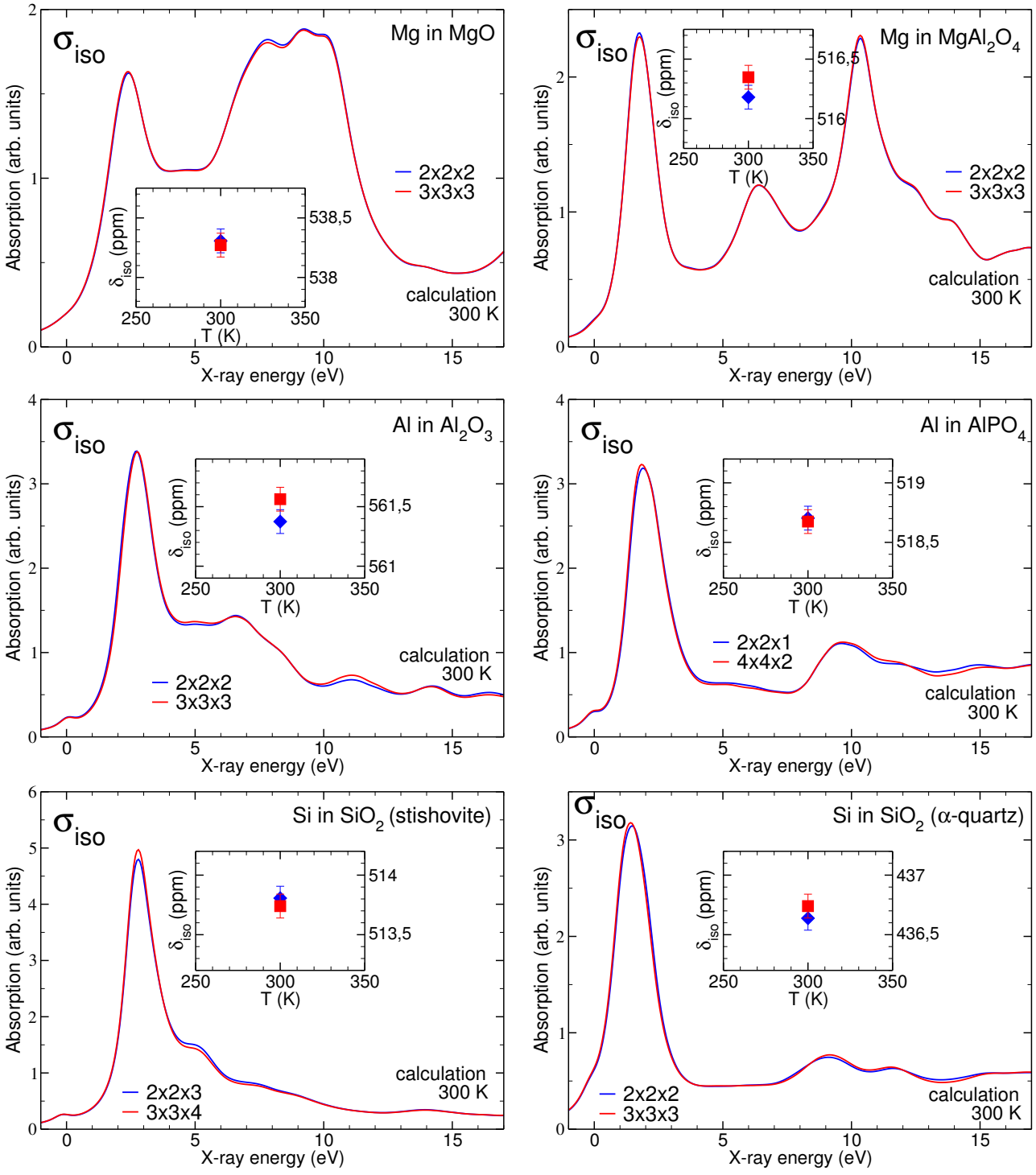

Figure 1: Finite size effects in XANES and NMR data computed at 300 K. For each dataset, the two largest supercell sizes considered are shown. The error bar for NMR calculation is about 0.1 ppm.

3 Quantum thermal saturation

The T_s quantum saturation temperature is related to the saturation phonon frequency Ω_s by $k_B T_s = \frac{1}{4}\hbar\Omega_s$, with k_B the Boltzmann constant (Table 3) [4].

Table 3: Saturation temperatures on NMR parameters obtained in mineral oxides from the QHA model. The coordination number of the probed atom is given between square brackets. Due to their small variations, it was impossible to fit α-Quartz data with an acceptable precision.

Atom	Compound	T_s (K)	Ω_s (cm^{-1})
Mg	Periclase (6)	277	770
	Spinel (4)	263	733
Al	Spinel (6)	276	767
	Corundum (6)	169	468
	Berlinite (4)	198	550
Si	Stishovite (4)	434	603
	α-Quartz (4)	/	/

4 NMR anisotropy parameters

In the Haeberlen convention [5], the principal values of δ are ordered such as $|\delta_{zz} - \delta_{\rm iso}| > |\delta_{xx} - \delta_{\rm iso}| > |\delta_{yy} - \delta_{\rm iso}|$. The chemical-shift anisotropy (CSA) is defined by its amplitude $\delta_{\rm CSA} = \delta_{zz} - \delta_{\rm iso}$ and its asymmetry parameter $\eta_{\rm CSA} = (\sigma_{xx} - \sigma_{yy})/(\sigma_{zz} - \sigma_{\rm iso})$. CSA is specific solid-state NMR since it is averaged by the molecular motion in liquid-phase NMR. The quadrupolar interaction is also anisotropic, with the quadrupolar asymmetry parameter $\eta_{\rm Q}$ defined as $\eta_{\rm Q} = (V_{xx} - V_{yy})/V_{zz}$.

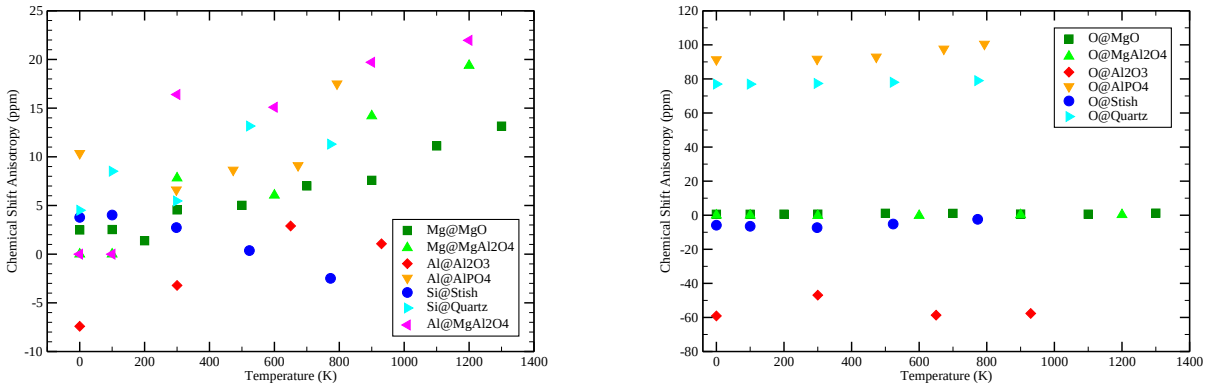

Figure 2: Temperature-dependence of the chemical-shift anisotropy of the cations (a) and oxygen atoms (b) in oxides.

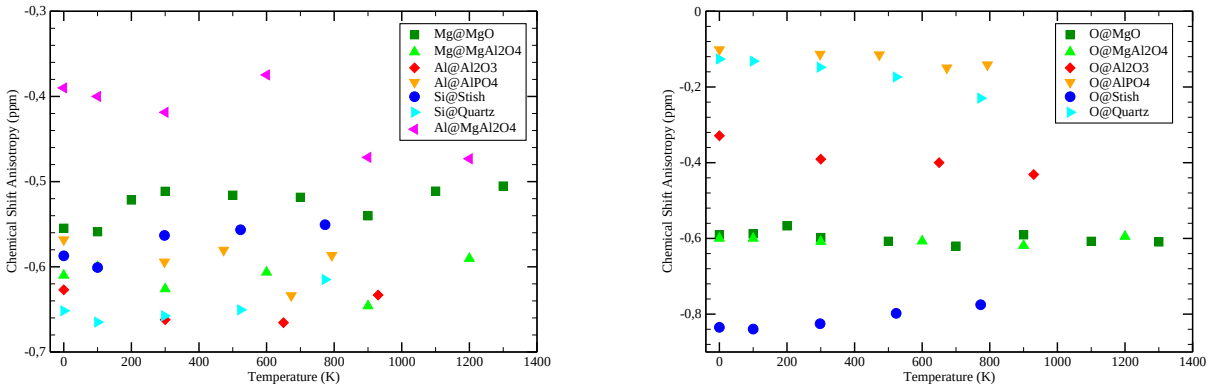

Figure 3: Temperature-dependence of the asymmetry parameter of the chemical-shift anisotropy for the cations (a) and oxygen atoms (b) in oxides.

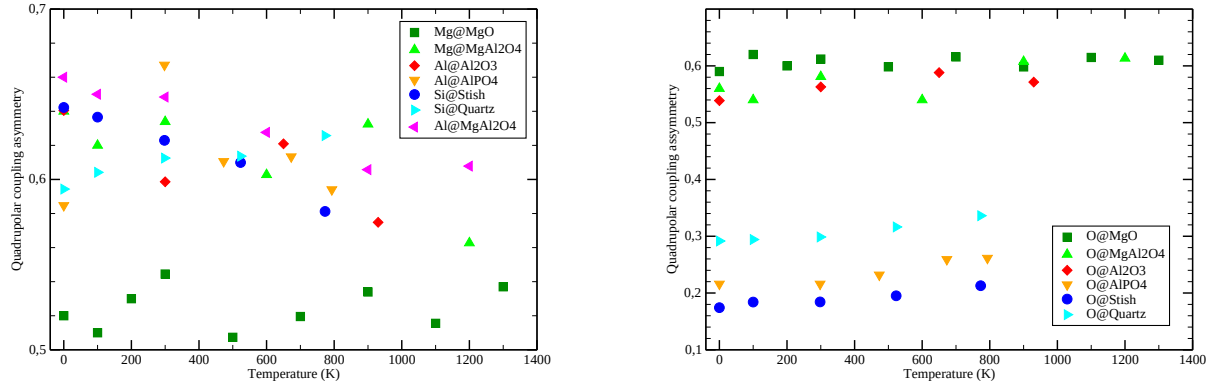

Figure 4: Temperature-dependence of the asymmetry parameter of the quadrupolar coupling for the cations (a) and oxygen atoms (b) in oxides.

Bibliography

[1] N. Troullier and J. L. Martins, *Phys. Rev. B: Condens. Matter Mater. Phys.*, 1991, **43**, 1993.

[2] X. Gonze and C. Lee, *Phys. Rev. B: Condens. Matter Mater. Phys.*, 1997, **55**, 10355.

[3] H. J. Monkhorst and J. D. Pack, *Phys. Rev. B: Condens. Matter Mater. Phys.*, 1976, **13**, 5188.

[4] E. Balan, S. Delattre, M. Guillaumet and E. K. H. Salje, *Am. Mineral.*, 2010, **95**, 1257–1266.

[5] U. Haeberlen, *High Resolution NMR in Solids: Selective Averaging*, Academic Press, New York, 1976, pp. 1–190.